A Fourier approach to diffraction of pulsed ultrasonic waves in lossless media

Daniel Guyomar and John Powers
Department of Electrical and Computer Engineering, Naval Postgraduate School, Monterey, California 93943

(Received 10 February 1986; accepted for publication 25 January 1987)

A method based on a Fourier domain approach is presented for computing the diffraction of a pulsed ultrasound wave from a rigidly baffled source in lossless media. The propagation from a planar source is dependent on the total impulse response which is just the Green's function. Computing the spatial transform of the point spread function gives the propagation transfer function which multiplies the spatial spectrum of the spatial excitation to produce the spatial spectrum of the propagated wave. The propagation transfer function can then be considered to be a time-varying spatial filter. The results are valid for separable arbitrary time excitation and planar spatial distributions of the source. The solution is amenable to including the effects of a finite receiver. Results of different simulations using this method are included.

PACS numbers: 43.20.Fn, 43.20.Px, 43.20.Bi

INTRODUCTION

Acoustic imaging and tissue characterization techniques require information about the insonifying wave at the object location in order to isolate the object's effects on the wave. While the propagation of monochromatic waves is well solved by the application of the angular spectrum technique[1] or Fresnel integrals, the propagation of a pulse of ultrasound with arbitrary temporal and spatial shape is less well understood. Others[2–15] have sought to find expressions for the field radiated from a baffled piston source into a lossless medium in various forms.

The approach followed here is based on the spatial impulse response method introduced by Stepanishen[4–7] and reviewed by Harris,[8] where the field is expressed as a temporal convolution of the time excitation with the spatial impulse response of the propagation. It differs from Stepanishen's work in that linear systems theory is used to point out the importance of the total impulse response (and its equivalence to the Green's function). Also, the expressions for the spatial impulse response functions are found in the spatial transform domain. In this domain, propagation of the wave is seen to be the application of a time-varying spatial filter to the spatial spectrum of the input wave.

I. THEORY

The problem that we wish to solve can be stated using the geometry of Fig. 1. Given the z-directed velocity excitation over an arbitrary shaped region of the $z=0$ plane, we wish to find the acoustic velocity potential $\phi(x,y,z,t)$ at an arbitrary point in the positive-z half-space. The region in the input plane will be assumed to be rigidly baffled. (It has been shown[13,14] to be possible to relate impedance-matched boundary conditions and resilient boundary conditions to the solutions for the rigid baffle.) We will assume that the time and space variations of the input z velocity are separable and that the z velocity is given by

$$v_z(x,y,0,t) = T(t)s(x,y) . \tag{1}$$

In the impulse response technique, it has been shown[4–8,12] that the relation between the acoustic potential and the input z velocity is

$$\phi(x,y,z,t) = T(t) \underset{t}{*} p(x,y,z,t) , \tag{2}$$

where the * symbol indicates convolution over the variable appearing immediately below it. The quantity $p(x,y,z,t)$ is known variously as the "impulse response,"[4,6,11] the "generalized impulse response,"[15] the "aperture impulse response,"[13] or the "spatial impulse response."[8,9] We will use the latter nomenclature and call $p(x,y,z,t)$ the spatial impulse response. The spatial impulse response is defined as the velocity potential that will result when the source is excited by a z velocity of the form $s(x,y)\delta(t)$, where δ is the Dirac impulse function. Hence, the problem of finding $\phi(x,y,z,t)$ is reduced to one of finding the spatial impulse response of the assumed spatial excitation.

Other approaches have been successful in computing the desired potential in lossless media using geometric interpretations of the integral limits and are reviewed in Ref. 8. More recent techniques include Refs. 13–15. Because of the geometrical interpretation of the limits the integrals do not lend themselves to rapid solution by efficient computer algorithms such as the FFT.

It should be noted that the problem posed where one knows the z-directed velocity can be referred to as the "source propagation problem" since the z-directed velocity is frequently assumed known in modeling transducers. The case where one knows the velocity potential in the input plane $\phi(x,y,0,t)$ could be characterized as the "field propagation problem" since it is characteristic of wave diffraction problems from one plane to another parallel plane. This diffraction problem can be readily cast into the form of a source propagation problem in the following manner.

A separable velocity potential at the input plane would be of the form

$$\phi(x,y,0,t) = s(x,y)\tau(t) . \tag{3}$$

 0001-4966/87/070354-06$00.80

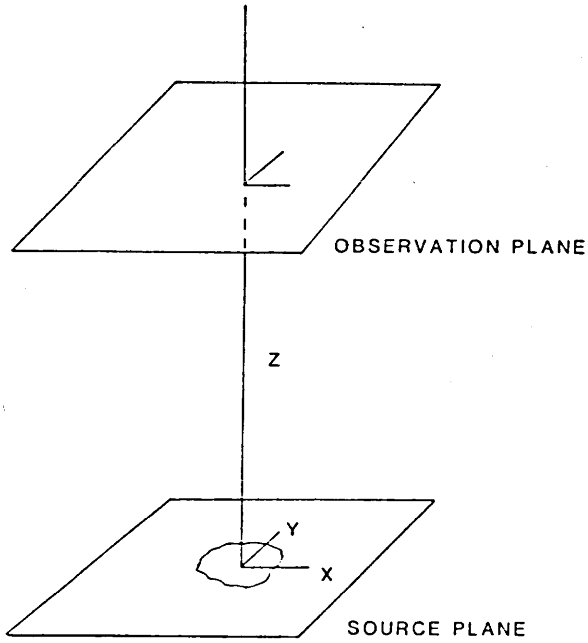

FIG. 1. Source and receiver geometry.

We want to convert this to an equivalent z-directed velocity distribution so that we can use Eq. (2) and the method to be described in this article. The relation between the z component of velocity and the velocity potential results from the relation

$$\mathbf{v}(x,y,z,t) = -\nabla\phi(x,y,z,t) . \tag{4}$$

Hence,

$$v_z(x,y,z,t) = -\frac{\partial\phi(x,y,z,t)}{\partial z} . \tag{5}$$

The wave given by Eq. (3) is planar and propagating in the $+z$ direction. As such, the argument of the traveling wave will be of the form $ct - z$, and the spatial z derivative is related to the temporal derivative by the operational relation

$$\frac{\partial}{\partial z} = -c\frac{\partial}{\partial t} . \tag{6}$$

Hence, we find that for a given $\phi(x,y,z,t)$ of the form of Eq. (3), the equivalent z-directed velocity is

$$v_z = -c\frac{\partial\phi(x,y,0,t)}{\partial t} \tag{7}$$

$$= -cs(x,y)\tau'(t) , \tag{8}$$

where τ' is the time derivative of $\tau(t)$. By comparison with the form Eq. (1) we would use $T(t) = -c\tau'(t)$ in the following equations for the solving the field propagation problem.

The spatial impulse response $p(x,y,z,t)$ is defined[4] as the response to a spatial excitation of the form $s(x,y)\delta(t)$. To find this response we use linear systems theory.[1] The *total impulse response* $h(x,y,z,t)$ of a system is represented as in Fig. 2(a). An impulsive input of the form $\delta(x,y)\delta(t)$ produces the total impulse response $h(x,y,z,t)$ at the observation plane. If the system is linear and space invariant (as is propagation in a linear homogeneous medium), then linear systems theory predicts[1] that the spatial impulse response $p(x,y,z,t)$ is related to the total impulse response $h(x,y,t)$ for a temporal impulsive input of the form $s(x,y)\delta(t)$ by the equation

$$p(x,y,z,t) = s(x,y)\underset{x\,y}{**}h(x,y,t) , \tag{9}$$

as shown in Fig. 2(b). Hence, to find the spatial impulse response in this approach, we need to first find the total impulse response of the system $h(x,y,z,t)$.

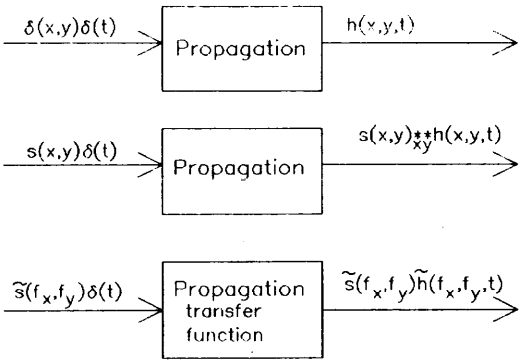

FIG. 2. (a) Propagation impulse response; (b) spatial impulse response; (c) spatial impulse response in the Fourier domain.

The total impulse response of the system is the propagation field resulting from a source at the input plane of the form $\delta(x,y)\delta(t)$ that solves the wave equation and meets the boundary condition. This solution is just the Green's function satisfying the wave equation and boundary conditions. Hence, we find that if the Green's function is known, one knows the total impulse response function.

The double spatial convolution in Eq. (9) over x and y is difficult to implement on a computer. To convert the convolutions to multiplications, we choose to enter the spatial frequency domain by taking the two-dimensional Fourier spatial transform of the system input and output. This is shown in Fig. 2(c) (where the tilde indicates the spatial Fourier transform of the function). Equation (9) then becomes

$$\tilde{p}(f_x,f_y,z,t) = \tilde{s}(f_x,f_y)\tilde{h}(f_x,f_y,t) . \tag{10}$$

The quantity $\tilde{h}(f_x,f_y,t)$ is the *propagation transfer function* and is the spatial transform of the total impulse response (or, equivalently, the spatial transform of the Green's function of the problem). Often, it is easier to find the propagation transfer function directly than it is to find the Green's function. For other cases, the Green's function can be found and the propagation transfer function computed by taking the spatial Fourier transform using FFT algorithms.

The technique, then, begins with a representation of the wave equation model. The Green's function that solves the wave equation and satisfies the assumed rigid baffle boundary conditions is then found, and the propagation transfer function computed by taking the spatial transform of the Green's function. (Alternatively, the propagation transfer function can sometimes be found directly from the equation and boundary conditions.) The spatial transform of the spatial input function $s(x,y)$ is computed and multiplied by the propagation transfer function as in Eq. (10). The inverse spatial transform of the product yields the spatial impulse response $p(x,y,z,t)$. The temporal convolution of Eq. (2) is then evaluated to find the desired velocity potential.

To check the correctness of the method, we wish to compare the results with those obtained by other techniques for lossless media. The wave equation is

$$\nabla^2\phi - \frac{1}{c^2}\frac{\partial^2\phi}{\partial t^2} = 0\,, \tag{11}$$

where c is the sound velocity in the medium. The equation is to be solved subject to the boundary condition that $v_z(x,y,0,t)$ is the known z-directed velocity over some region of the source plane at $z = 0$. It is assumed that the velocity of the source is 0 outside of this region (i.e., that the source is in a rigid baffle) and that the potential meets the Sommerfeld radiation conditions[1] as the distance goes to infinity. The geometry is illustrated in Fig. 1. The acoustic velocity vector is easily related to the acoustic velocity potential by finding the negative of the gradient of the potential.

The Green's function for the rigid baffle is known[16] to be (assuming only outward traveling waves)

$$g(x,y,z,t) = \delta(ct - R)/2\pi R\,, \tag{12}$$

where $R = \sqrt{x^2+y^2+z^2}$. The spatial impulse response of this problem is

$$p(x,y,z,t) = 2s(x,y)\underset{xy}{**}\{\delta[t-(R/c)]/2\pi R\}\,. \tag{13}$$

We take the spatial transform of Eq. (12) to find the propagation transfer function $\tilde{h}_{p1}$ for lossless media as

$$\tilde{h}_{p1} = 2J_0(\rho\sqrt{c^2t^2-z^2})H(ct-z)\,, \tag{14}$$

where $\rho = 2\pi\sqrt{f_x^2+f_y^2}$ and $H(t)$ is the step function.

Since the results are going to be computer implemented and normalized to maximum values, we will drop the multiplicative constants. From Eq. (10), we know that the spatial transform $\tilde{h}$ of the spatial impulse response is given by the product of $\tilde{s}$ (the spatial transform of the input velocity spatial function) and the propagation transfer function $\tilde{h}_{p1}$. In this form we can identify the $J_0(\rho\sqrt{c^2t^2-z^2})H(ct-z)$ term as a time-varying multiplicative spatial filter for the propagation in lossless media from a source in a rigid baffle. The high spatial frequencies are attenuated compared to the lower spatial frequencies. As time increases, the Bessel function contracts causing a generally increased attenuation of the high spatial frequencies.

To check the validity of the technique we consider a circular piston producing an acoustic potential of radius a driven with a Dirac impulse time excitation (i.e., we will find the spatial impulse response of a uniform piston). References 2–11 and 13 have studied this problem. The transform of the spatial dependence of the source is

$$\tilde{s}(f_x,f_y) = aJ_1(\rho a)/\rho \tag{15}$$

and upon substitution into Eq. (14), the solution for the spatial impulse response is rediscovered[11] as

$$p(r,z,t) = kH(ct-z)\int_0^\infty J_1(\rho a) \times J_0(\rho\sqrt{c^2t^2-z^2})J_0(\rho r)d\rho\,, \tag{16}$$

where, for convenience, k represents the multiplicative constants. The integral is evaluated with the Sonine–Dougall formula[16] to give

for $r<a$

$$p(r,z,t) = \begin{cases} \text{const} & z<ct<\sqrt{z^2-(a-r)^2}, \\ \dfrac{k}{\pi}\cos^{-1}\left(\dfrac{c^2t^2-z^2+r^2-a^2}{2r\sqrt{c^2t^2-z^2}}\right) & \sqrt{z^2+(a-r)^2}<ct<\sqrt{z^2+(a+r)^2}, \\ 0 & ct>\sqrt{z^2+(a+r)^2}. \end{cases} \tag{17}$$

for $r>a$

$$p(r,z,t) = \begin{cases} 0 & z<ct<\sqrt{z^2-(a-r)^2} \\ \dfrac{k}{\pi}\cos^{-1}\left(\dfrac{c^2t^2-z^2+r^2-a^2}{2r\sqrt{c^2t^2-z^2}}\right) & \sqrt{z^2+(a-r)^2}<ct<\sqrt{z^2+(a+r)^2}, \\ 0 & ct>\sqrt{z^2+(a+r)^2}. \end{cases} \tag{18}$$

Within the neglected multiplicative constants, these results agree with those obtained by other techniques in Refs. 2–4, 7, 10, and 11, thereby confirming the technique of using the spatial frequency domain as in Eq. (14).

II. NUMERICAL SIMULATIONS

An additional advantage to the spatial spectrum approach discussed here beyond the physical interpretation of the propagation as a time-varying spatial filter is that the solutions are readily amenable to numerical solutions through the use of FFT routines and Fourier–Bessel algorithms[18] for circularly symmetric geometries. To illustrate numerical solutions we consider some cases. The following simulations have been done using a 64×64 array of data.

While the method gives a three-dimensional solution at any observation distance, one dimension is eliminated in the plots by representing the solution through a median of the source. The plots show the amplitude of the wave plotted against cross direction and time. For plotting convenience, the following plots have been normalized to the maximum amplitude value. The spatial axis is normalized to the characteristic source size D (i.e., either the diameter or the width of the source), and the time axis is normalized by the value of D/c. The origin of the time axis begins at z/c, the instant that the first part of the wave arrives at the observation plane. All plots are in an observation plane located 10 cm in front of the source plane. (These simulation results have been previously published in an unrefereed conference proceedings.[17])

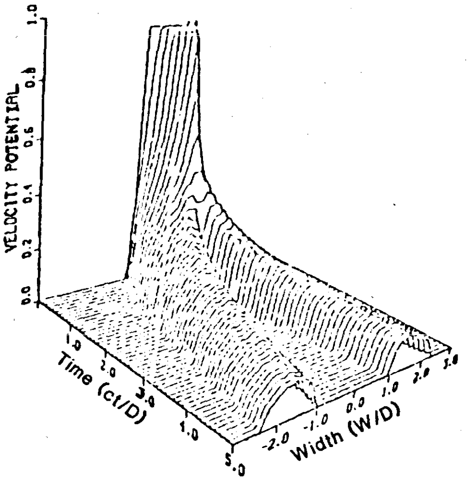

FIG. 3. Lossless propagation of circular piston ($D = 2.2$ cm), impulse excitation, $z = 10$ cm.

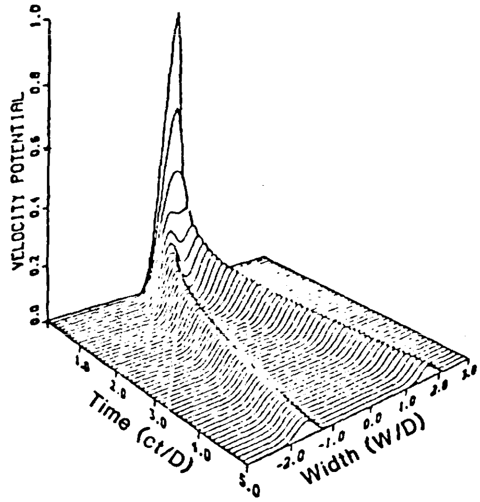

FIG. 5. Lossless propagation from a truncated Gaussian wave ($1/e$ point is 0.491 cm from center), impulse excitation, $z = 10$ cm.

A. Case 1. Impulse excitation

Equation (14) gives the transform of the spatial impulse response. With the help of an FFT algorithm, we can obtain the source spatial spectrum multiplied by the propagation transfer function. Then a 2-D inverse FFT is applied to get the field at a given time. For a radially symmetric case, the FFTs can be replaced by a faster Hankel transform algorithm.[18] One of the features of the technique is that the method does not require specific sampling in time or distance z so the field can be computed anywhere or at any instant of time without requiring large amounts of computer time.

Figure 3 shows the diffraction pattern from a circular transducer (the diameter is $D = 2.2$ cm) excited by an impulse as observed on the axis, $x = 0$. At $t = z/c$ the potential is replica of the excitation. As time progresses, the potential is a combination of waves from various points on the source. Late in time two distinct "tails" are observed and were explained in terms of edge waves in Ref. 3.

Figure 4 is a similar impulse excitation, but for a square transducer that is 2.2 cm on a side. The observation point is the same distance from the source.

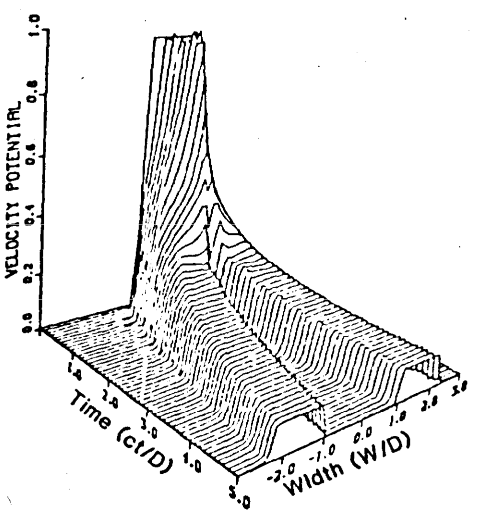

FIG. 4. Lossless propagation of square transducer ($D = 2.2$ cm), impulse excitation, $z = 10$ cm.

In Fig. 5, the pattern is shown for an axisymmetric Gaussian shaped wave with an impulse time excitation. The $1/e$ point is $1.1/\sqrt{5}$ cm from the center with the observation point kept the same as in the previous figures. The shape of the Gaussian wave stays much the same because of the low spatial frequency content of this waveshape. Only large values of time cause substantial spatial filtering for these low spatial frequencies.

B. Case 2. Arbitrary time excitation

For a time excitation different than $\delta(t)$, the diffracted wave is a convolution between the spatial impulse response and the temporal excitation portion of the source acoustic potential, as given by Eq. (2). Figure 6(a) is the circular transducer of Fig. 3 (the diameter is 2.2 cm) excited by a constant amplitude pulse of 10-μs duration for a lossless medium. The smoothing effect of the time-domain convolution is evident along the propagation direction. Figure 6(b) is the same transducer excited by one cycle of square wave with a 12-μs period. We now note a more complicated behavior with a noticeable time delay before reaching the maximum amplitude on-axis and an apparent differentiation across the width dimension. [Figure 6(a) also has a time delay but this time delay is less noticeable.]

C. Case 3. Finite receiver effects

A receiver which is not a point receiver will perturb the observed field in the way that it averages the field. This averaging effect can be included in this method. The spatial frequency domain is well suited to include these effects since the receiver contributes another low-pass spatial filter.

The averaged field can be written as

$$\langle \phi(x,y,z,t) \rangle = \int_S \phi(x - x_i, y - y_i, z, t) \times A(x_i, y_i) dx_i \, dy_i , \tag{19}$$

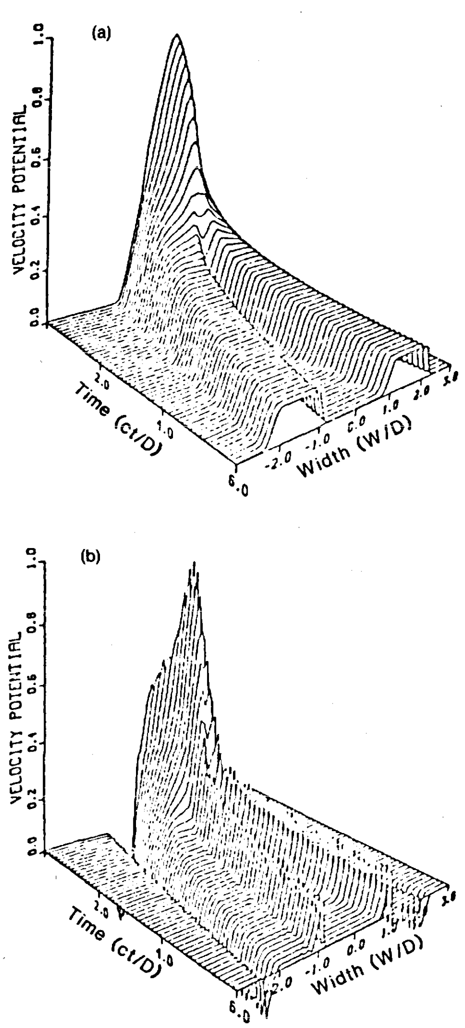

FIG. 6. Diffracted wave for nonimpulse excitation of a circular transducer, $z = 10$ cm. (a) Rectangular pulse excitation ($T = 10^{-5}$ s). (b) Square wave (one cycle) excitation ($T = 1.2 \times 10^{-5}$ s).

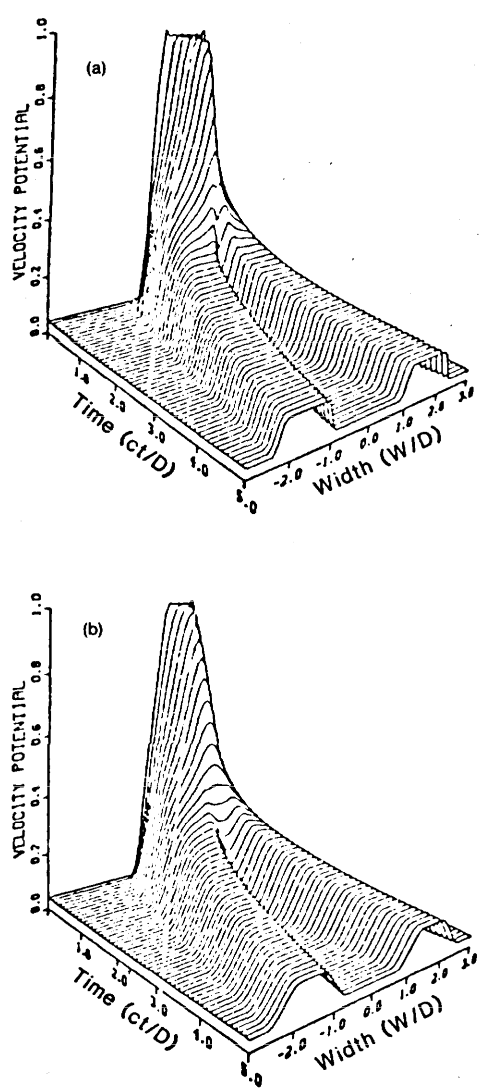

FIG. 7. Impulse response measured with finite size receiver. Circular source ($D = 2.2$ cm), circular receiver, lossless medium, $z = 10$ cm. (a) Receiver radius $= 1/2\pi$ cm. (b) Receiver radius $= 3/2\pi$ cm.

where S is the surface of the receiver and $A(x_i,y_i)$ is the receiver sensitivity. The above average is a two-dimensional spatial convolution or a simple product in the spatial frequency domain. Thus the receiving transducer is modeled in the spatial frequency domain as a multiplicative spatial filter given by $\widetilde{A}(f_x,f_y)$. The response for an impulse-excited transducer as measured at the receiver is

$$\langle \phi(x,y,z,t) \rangle = \mathscr{F}^{-1}\left[\tilde{s}(f_x,f_y) \widetilde{A}\,(f_x,f_y) J_0\left(\rho\sqrt{c^2t^2 - z^2}\right) \right] \times H(ct - z)\,, \tag{20}$$

where $\mathscr{F}^{-1}[\bullet]$ is the inverse two-dimensional transform operator. Figure 7 shows the detected field for receivers of different size. The source is the circular transducer used in Fig. 3. The spatial convolution effect of the receiver is seen in the slight slope of the edge waves.

III. SUMMARY

This article presents a computationally efficient method of computing the transient acoustic waves in lossless media. The fields are expressed in terms of the spatial impulse response which is found by inverse transforming the product of the transform of the spatial excitation and the propagation transfer function. The propagation transfer function has been shown to be the transform of the Green's function which is the total impulse response of the propagation problem. No assumptions of the paraxial nature or restrictions on the propagation distance have been made. Additionally, the solutions in the space domain use the computationally efficient Fourier transform. Once the spatial impulse response is known, Eq. (2) can be used to find the field for an arbitrary time excitation and Eq. (20) can be used to incorporate the results of a finite aperture receiver. Several numerical simulations have been given to illustrate the results of the technique.

ACKNOWLEDGMENTS

This work was partially supported by the Foundation Research Program of the Naval Postgraduate School. Daniel Guyomar was a Research Associate of the National Research Council and is now with Schlumberger-EPS in Clamart, France.

[1]See, for example, J. W. Goodman, *Introduction to Fourier Optics* (McGraw-Hill, New York, 1969).
[2]F. Oberhettinger, "On transient solutions of the 'baffled piston' problem," J. Nat. Bur. Stand. **65** B, 1–6 (1961).
[3]G. E. Tupholme, "Generation of acoustic pulses by baffled plane pistons," Mathematika **16**, 209–224 (1969).
[4]P. R. Stepanishen, "Transient radiation from pistons in an infinite planar baffle," J. Acoust. Soc. Am. **49**, 1629–1637 (1971).
[5]P. R. Stepanishen, "Acoustic transients in the far-field of a baffled circular piston using the impulse response approach," J. Sound Vib. **32**, 295–310 (1974).
[6]P. R. Stepanishen, "Acoustic transients from planar axisymmetric vibrators using the impulse response method," J. Acoust. Soc. Am. **70**, 1176–1181 (1981).
[7]P. R. Stepanishen and G. Fisher, "Experimental verification of the impulse response method to evaluate transient acoustic fields," J. Acoust. Soc. Am. **69**, 1610–1617 (1981).
[8]G. R. Harris, "Review of transient field theory for a baffled planar piston," J. Acoust. Soc. Am. **70**, 10–20 (1981).
[9]G. R. Harris, "Transient field of a baffled piston having an arbitrary vibration amplitude distribution," J. Acoust. Soc. Am. **70**, 186–204 (1981).
[10]J. C. Lockwood and J. G. Willette, "High speed method for computing the exact solution for the pressure variations in the nearfield of a baffled piston," J. Acoust. Soc. Am. **53**, 735–741 (1973).
[11]M. Greenspan, "Piston radiator: Some extensions of the theory," J. Acoust. Soc. Am. **65**, 608–621 (1979).
[12]J. Weight and A. Hayman, "Observation of the propagation of very short ultrasonic pulses and their reflection by small targets," J. Acoust. Soc. Am. **63**, 396–404 (1978).
[13]H. Lasota, R. Salamon, and B. Delannoy, "Acoustic diffraction analysis by the impulse response method: A line impulse response approach," J. Acoust. Soc. Am. **76**, 280–290 (1984).
[14]D. Guyomar and J. Powers, "Boundary effects on transient radiation fields from vibrating surfaces," J. Acoust. Soc. Am. **77**, 907–915 (1985).
[15]A. F. Medeiros and P. R. Stepanishen, "The forward and backward projection of acoustic fields from axisymmetric ultrasonic radiators using impulse response and Hankel transform techniques," J. Acoust. Soc. Am. **75**, 1732–1740 (1984).
[16]P. M. Morse and K. U. Ingard, *Theoretical Acoustics* (McGraw-Hill, New York, 1968), p. 369.
[17]D. Guyomar and J. Powers, "A Fourier approach to diffraction of pulsed ultrasonic waves in lossless media," in *1985 Ultrasonics Symposium Proceedings*, edited by B. R. McAvoy (Institute of Electrical and Electronic Engineers, New York, 1985), pp. 692–695.
[18]S. Candel, "An algorithm for the Fourier–Bessel transform," Comput. Phys. Commun. **23**, 343–353 (1981).